1   **Iron-sulfur cluster repair contributes to *Y. pseudotuberculosis* survival within deep tissues.**

2

3

4   Running title: Iron-sulfur cluster repair during *Y. pseudotuberculosis* infection

5

6

7

8   Kimberly M. Davis[1,#a,*], Joanna Krupp[1], Stacie Clark[1,2], Ralph R. Isberg[1]

9
10
11
12   [1]Department of Molecular Biology and Microbiology
13   [2]Graduate Program in Molecular Microbiology
14   Tufts University School of Medicine, Boston, MA, USA
15   [#a]Current Address: W. Harry Feinstone Department of Molecular Microbiology and Immunology
16   Johns Hopkins Bloomberg School of Public Health, Baltimore, MD, USA
17
18
19
20
21

22   *Corresponding author:

23   E-mail: kdavi140@jhu.edu (KMD)
24

25 **Abstract**

26 To successfully colonize host tissues, bacteria must respond to and detoxify many different host-

27 derived antimicrobial compounds, such as nitric oxide (NO). NO has direct antimicrobial

28 activity through attack on iron-sulfur (Fe-S) cluster-containing proteins. NO detoxification plays

29 an important role in promoting bacterial survival, but it remains unclear if repair of Fe-S clusters

30 is also important for bacterial survival within host tissues. Here we show that the Fe-S cluster

31 repair protein, YtfE, contributes to the survival of *Y. pseudotuberculosis* within the spleen

32 following nitrosative stress. *Y. pseudotuberculosis* forms clustered centers of replicating bacteria

33 within deep tissues, where peripheral bacteria express the NO-detoxifying gene, *hmp*. *ytfE*

34 expression also occurred specifically within peripheral cells at the edges of microcolonies. In the

35 absence of *ytfE*, the area of microcolonies was significantly smaller than WT, consistent with

36 *ytfE* contributing to the survival of peripheral cells. The loss of *ytfE* did not alter the ability of

37 cells to detoxify NO, which occurred within peripheral cells in both WT and Δ*ytfE*

38 microcolonies. In the absence of NO-detoxifying activity by *hmp*, NO diffused across Δ*ytfE*

39 microcolonies, and there was a significant decrease in the area of microcolonies lacking *ytfE*,

40 indicating that *ytfE* also contributes to bacterial survival in the absence of NO detoxification.

41 These results indicate a role for Fe-S cluster repair in the survival of *Y. pseudotuberculosis*

42 within the spleen, and suggest that extracellular bacteria may rely on this pathway for survival

43 within host tissues.

Introduction

44

45   Nitric oxide (NO) is a diffusible gas that has a wide range of physiological functions

46   within mammals (1, 2). The effects of NO are tissue concentration-dependent, as it promotes

47   vasodilation, cell proliferation and cell differentiation at low concentrations (3, 4), while high

48   concentrations drive apoptosis and defense against bacterial, fungi, and parasites (5-8). NO is

49   produced by three different nitric oxide synthase (NOS) isoforms within mammalian tissues: the

50   neuronal NOS (nNOS), endothelial NOS (eNOS), and inducible NOS (iNOS). nNOS and eNOS

51   are expressed at low levels by endothelial and neuronal cells respectively (2). In contrast, iNOS

52   is expressed by a wide range of cell types, specifically in response to NF-κB-dependent sensing

53   of, and is responsible for the high levels of NO produced during infection (1, 9).

54   NO has direct antimicrobial activity and can also react with reactive oxygen species to

55   produce additional toxic compounds, such as peroxynitrite. NO may be bacteriostatic, while

56   peroxynitrite is known to have direct bactericidal activity (10). NO antibacterial activity occurs

57   through nitrosylation of iron-sulfur (Fe-S) cluster-containing proteins, which play critical roles in

58   cellular respiration, DNA synthesis, and gene regulation. NO also targets heme groups, reactive

59   thiols, tyrosyl radicals, and can cause DNA damage (1, 10). One of the global regulators in *E.*

60   *coli* that has been shown to be inactivated by NO is NsrR (11), which regulates the response to

61   nitrosative stress and is also associated with the oxidative stress response (12-14). Nitrosylation

62   of the NsrR-associated Fe-S cluster relieves repression of at least 60 genes in *E. coli* (15-18).

63   Included in this regulon is the *hmp* gene, which encodes a flavohemoglobin that detoxifies NO

64   (19, 20), and YtfE (also known as Repair of Iron Centers (RIC) in *E. coli*), which functions to

65   repair Fe-S clusters following NO damage (13, 17). Repair of Fe-S cluster proteins by YtfE can

66   eliminate the need for new Fe-S cluster biogenesis when Fe availability is limited (13, 21, 22). A

3

67   variety of studies argue that YtfE contributes to bacterial survival within host cells, but it remains

68   unclear if YtfE contributes to the survival of extracellular pathogens replicating within host

69   tissues, and if YtfE contributes to survival following exposure to NO (23-25).

70   *Yersinia pseudotuberculosis* is an oral pathogen that is typically contained within

71   intestinal tissues and gut-associated lymphoid tissues, but has the capacity to spread systemically

72   in susceptible individuals (26-29). Following bloodstream access, *Y. pseudotuberculosis*

73   colonizes deep tissue sites where individual bacteria replicate to form clonal microcolonies (30-

74   32). Neutrophils, monocytes, and macrophages are recruited to sites of bacterial replication,

75   which are kept at bay by *Yersinia*, primarily via substrates of the bacterial type III secretion

76   system (33-35). Recruited monocytes and macrophages produce NO, which diffuses across a

77   layer of neutrophils and is inactivated at the periphery of the microcolony by bacteria expressing

78   Hmp, preventing diffusion of NO into the interior of the microcolony (32). The consequences of

79   the selective attack of NO on the peripheral bacteria are unclear, although it is likely that

80   nitrosative stress may slow their growth. Additional members of the nitrosative stress response,

81   such as YtfE, may also be required in peripheral cells to ensure their survival.

82   Bacteria responding to RNS appear to recover and remain viable, consistent with

83   members of the NsrR regulon cooperating to repair NO-mediated damage in peripheral bacteria

84   within microcolonies. Two of the members of the *E. coli* NsrR regulon, *hmp* and *ytfE,* are

85   upregulated in the bubonic plague model of *Yersinia pestis* infection and during Peyer's patch

86   colonization by *Y. pseudotuberculosis* (36, 37). The similar expression patterns of *hmp* and *ytfE*

87   may suggest that both genes are also members of the NsrR regulon in *Yersinia,* and could both

88   contribute to microbial fitness during microcolony growth. Additionally, very few studies have

89   explored the role of Fe-S cluster repair during infection with extracellular bacteria. Here, we

90   show that *ytfE* contributes to the survival of extracellular bacteria, specifically through

91   upregulation of *ytfE* within peripheral cells of *Y. pseudotuberculosis* microcolonies.

92   **Results.**

93   ***Y. pseudotuberculosis ytfE* expression is regulated by NsrR and occurs within peripheral**

94   **cells during growth in the spleen.**

95   The *ytfE* gene is known to be a member of the NsrR regulon in a number of bacterial

96   species (13, 14, 38), so *ytfE* is expected to be repressed by NsrR in *Y. pseudotuberculosis*. We

97   also expected that *ytfE* is transcribed during *Y. pseudotuberculosis* growth within the mouse

98   spleen as the NsrR-regulated *hmp* gene is expressed in this tissue (23-25, 32, 36). To determine if

99   *Y. pseudotuberculosis ytfE* is expressed during splenic growth, C57BL/6 mice were intravenously

100   challenged with bacteria and bacterial RNA was isolated at day 3 post-inoculation (PI). Based on

101   qRT-PCR analysis, *ytfE* transcript levels increased within the mouse spleen relative to the

102   inoculum culture grown in the absence of an NO-generating system, with marked mouse-to-

103   mouse variation (Figure 1A) (32).   To determine if *ytfE* expression is NsrR-dependent, we

104   compared *ytfE* transcription levels in WT and Δ*nsrR* strains in the presence (+) and absence (-) of

105   nitrogen stress imparted by acidified nitrite (NO_2). Transcription of *ytfE* increased by over 100X

106   in the WT strain with the addition of nitrogen stress (Figure 1B). Transcription of *ytfE* was high

107   in the Δ*nsrR* strain in either the presence or absence of nitrogen stress, indicating that NsrR

108   negatively regulates *ytfE* transcription. A slight increase in *ytfE* expression in the Δ*nsrR* strain

109   with nitrogen stress suggests additional pathways may regulate *ytfE* expression.

110   Hmp, another member of the NsrR regulon, is specifically expressed on the periphery of

111   *Y. pseudotuberculosis* microcolonies during splenic growth (32). At the transcriptional level,

112   this is associated with considerable variation in expression levels between individual mice.

113   Variation is likely due to the presence of different size microcolonies within different organs, as

114   distinct peripheral expression of *hmp* is visualized in large microcolonies, and smaller

6

115   microcolonies are more homogenous. The variable *ytfE* expression levels in the mouse and

116   NsrR-dependence is reminiscent of *hmp* expression, indicating that there could be a link between

117   spatial expression and inter-mouse variation. To determine if *ytfE* and *hmp* have similar

118   expression patterns during growth in the spleen, mice were intravenously inoculated with a WT

119   *Y. pseudotuberculosis* strain containing *hmp::mCherry* (chromosomal integration of *mCherry*

120   downstream of *hmp*) and *ytfE::gfp* (chromosomal integration of *gfp* downstream of *ytfE*).

121   Microcolonies were visualized within the spleen using fluorescence microscopy, and *ytfE* and

122   *hmp* reporter signals were quantified within the same cells at the center and periphery of the

123   microcolonies (Materials and Methods). The *hmp* reporter signal increased within individual

124   cells at the periphery relative to cells at the centroid of microcolonies, which generated a ratio

125   value greater than 1, consistent with *hmp* peripheral expression (Figure 1C). The *ytfE* signal was

126   dim relative to *hmp*, but also increased at the periphery of microcolonies relative to the centroid.

127   The Periphery/Centroid signal intensity ratio value for *ytfE* was similar to *hmp*, indicating that

128   *ytfE* was expressed at the periphery of microcolonies (Figure 1C). To confirm the dim *ytfE*

129   signal was not due to mCherry fluorescence detected in the gfp channel, experiments were also

130   performed in a WT strain containing *yopE::mCherry* and *ytfE::gfp*. *yopE* and *ytfE* exhibited

131   distinct reporter patterns indicating the detected gfp signal was due to *ytfE* reporter expression

132   (Figure 1C, 1D). There was significant overlap in the *hmp* and *ytfE* signals within these images,

133   and based on NsrR-dependent regulation of both genes, it is likely that *hmp* and *ytfE* were

134   expressed in the same cells (Figure 1D).

135   **_ytfE_ contributes to the virulence of _Y. pseudotuberculosis_ in the spleen.**

136   YtfE repairs Fe-S clusters damaged by NO, and there appears to be sufficient NO at the

137   periphery of splenic microcolonies to allow synthesis of this protein and to promote repair within

7

138   this subpopulation of bacteria. To determine if loss of *yftE* alters the overall fitness of *Y.*

139   *pseudotuberculosis* during growth within the spleen, we constructed a *Y. pseudotuberculosis*

140   strain that lacks the *ytfE* gene (Δ*ytfE*) and harbors a constitutive *gfp*-expressing plasmid, to

141   visualize growth within the spleen. To compare differences in relative fitness, mice were

142   infected intravenously with equal amounts of WT mCherry$^+$ and Δ*ytfE* GFP$^+$ strains, and spleens

143   were harvested at day 3 PI, a late stage of infection in this model, to determine the competitive

144   index by colony forming units (CFUs) and quantify microcolony areas within the same animals.

145   At day 3 PI, the median competitive index was significantly less than 1, indicating lowered

146   fitness of the Δ*ytfE* strain relative to the WT strain (Figure 2A; p=0.0115). The areas of

147   individual microcolonies within these co-infected tissues were also visualized and quantified by

148   fluorescence microscopy in 11 mice. The Δ*ytfE* microcolonies were significantly smaller than

149   WT microcolonies within the same organs, indicating that *ytfE* contributes to the survival of *Y.*

150   *pseudotuberculosis* in the spleen, presumably due to lowered fitness of the bacterial population

151   located at the periphery of the microcolonies (Figure 2B).

152   Since YtfE could directly repair the Fe-S cluster of NsrR, the absence of *ytfE* could alter

153   expression of the NsrR regulon, by resulting in heightened expression within peripheral cells. To

154   determine if microcolonies from the *Y. pseudotuberculosis* Δ*ytfE* strain have sustained

155   expression of the NsrR regulon relative to the WT strain, we infected mice intravenously with

156   WT GFP$^+$ *hmp::mCherry* or Δ*ytfE* GFP$^+$ *hmp::mCherry* integrated *hmp* reporter strains, and

157   spleens were harvested at day 3 PI to visualize reporter expression by fluorescence microscopy.

158   Similar to Fig. 1D, *hmp* reporter expression was significantly higher at the periphery relative to

159   the centroid in the WT strain (Figure 2C). The reporter expression pattern was very similar in

160   Δ*ytfE* microcolonies, indicating that there was still a gradient of NO exposure in the mutant, in

8

161   which Hmp activity in the peripheral population protects the central population of bacteria, and

162   that loss of *ytfE* did not significantly alter expression of the NsrR regulon (Figure 2D).

163   ***ytfE* contributes to bacterial survival in the absence of *hmp*.**

164   YftE contributed to the growth of *Y. pseudotuberculosis* microcolonies in the spleen

165   despite expression limited to the microcolony periphery. We were then interested in determining

166   if YtfE-mediated repair played an important role in the context of a Δ*hmp* strain, where all

167   bacteria in a microcolony are exposed to NO (32). To address this point, we challenged mice

168   intravenously with Δ*hmp* GFP$^+$ P_{hmp}::*mCherry* and Δ*hmp* Δ*ytfE* GFP$^+$ P_{hmp}::*mCherry* strains, and

169   spleens were harvested at day 3 PI to quantify CFUs, visualize microcolony areas, and detect

170   reporter signals by fluorescence microscopy. The Δ*hmp* Δ*ytfE* strain showed no potentiation of

171   the defect in single strain infections, but this defect can be observed during co-infection. The

172   median competitive index (CI) value for the double mutant was below 1, but was not

173   significantly less than 1, which suggests that Δ*hmp* Δ*ytfE* strain may not be less fit than Δ*hmp*

174   (Figure 3A). Interestingly, in 4 mice the CI was at least 1, indicating that the Δ*hmp* Δ*ytfE* strain

175   could compete efficiently with Δ*hmp* in these animals. We then compared the total CFU in the

176   organs in mice in which the Δ*hmp* strain outcompeted Δ*hmp* Δ*ytfE*, or in mice in which no such

177   outcompetition took place (Figure 3B). The total CFUs were significantly lower in organs in

178   which the Δ*hmp* did not outcompete the Δ*hmp*Δ*ytfE* strain, indicating that the fitness differences

179   were suppressed in animals showing increased restriction of bacterial growth. It is also possible

180   that the Δ*hmp*Δ*ytfE* strain had reduced levels of initial seeding within tissues. The microcolony

181   areas were quantified within all the spleens depicted in Figure 3A, and the areas of Δ*hmp* Δ*ytfE*

182   microcolonies were significantly smaller than Δ*hmp* (Figure 3C). Δ*hmp* Δ*ytfE* microcolonies had

183   similar P_{hmp} reporter expression at the centroid and periphery, indicating NO diffused across

9

184   these centers (Figure 3D). Together, these results confirm that *ytfE* contributes to bacterial

185   survival in the absence of Hmp detoxifying activity.

186   **ytfE has limited effects on NO sensitivity in the absence of *hmp***

187   The Δ*ytfE* single mutant strain had reduced fitness relative to the WT strain (Figure 2),

188   however the single Δ*ytfE* mutant was not significantly more sensitive than the WT strain to the

189   presence of acidified nitrite during growth in culture. Similarly, despite the lowered fitness of the

190   Δ*hmp* Δ*ytfE* strain in spleens relative to Δ*hmp*, the Δ*hmp* Δ*ytfE* strain was not significantly more

191   sensitive than the Δ*hmp* mutant strain to the presence of acidified nitrite during growth in culture

192   (Figure 4A; compare +NO$_2$ samples). The absence of *ytfE* also did not significantly alter the

193   sensitivity of strains to the NO donor compound, DETANONOate, during growth in minimal

194   media (Figure 4B). This is consistent with previous reports in other organisms (38, 39), perhaps

195   due to the presence of other backup repair pathways that are active in the absence of Hmp or

196   because YtfE plays a role in protection from other stress species.

197   We then compared *hmp* reporter expression in Δ*ytfE* and Δ*hmp*Δ*ytfE* strains to confirm

198   that NO diffusion occurred across Δ*hmp* Δ*ytfE* microcolonies using plasmid-borne reporters.

199   Mice were infected intravenously with Δ*ytfE* GFP$^+$ P$_{hmp}$::*mCherry* or Δ*hmp* Δ*ytfE* GFP$^+$

200   P$_{hmp}$::*mCherry* strains, and spleens were harvested 3 days PI to visualize reporter expression by

201   fluorescence microscopy. The Δ*ytfE* strain had peripheral P$_{hmp}$ reporter expression, as seen with

202   the chromosomally-integrated *hmp* reporter, indicating that NO diffusion across the microcolony

203   is inhibited by peripheral cells in Δ*ytfE* microcolonies (Figure 4C, 4D). Δ*hmp* Δ*ytfE*

204   microcolonies showed no such preference for the periphery, indicating NO diffused across these

205   centers, as expected based on the loss of *hmp*.

206   **Rescue of *ytfE* restores microcolony size.**

10

207   To show that the loss of *ytfE* was responsible for decreased microcolony size, we rescued

208   the Δ*ytfE* strain with a WT copy of *ytfE*, and transformed the *ytfE* rescued strain with the

209   constitutive *gfp*-expressing plasmid. Mice were infected intravenously with WT mCherry$^+$ and

210   *ytfE* rescued GFP$^+$ strains, and spleens were harvested at day 3 PI to quantify CFUs and visualize

211   microcolony areas by fluorescence microscopy. The median competitive index for the *ytfE*

212   rescued strain was close to a value of 1, indicating the fitness of this strain was roughly

213   equivalent to the WT strain (Figure 5A). The microcolony areas were quantified within all the

214   spleens depicted in Figure 5A, and the areas of *ytfE* rescued microcolonies were very similar to

215   WT microcolonies (Figure 5B, 5C). These results indicate that the Δ*ytfE* strain was rescued by

216   the WT copy of *ytfE*, which confirms that the reduced fitness of the Δ*ytfE* strain was specifically

217   due to a loss of *ytfE*.

11

Discussion

218

219   The detoxification of NO and other reactive nitrogen species is critical for bacterial

220   survival within host tissues (40-43). Bacterial proteins involved in NO detoxification, however,

221   are not synthesized until NO accumulates and damages the Fe-S clusters of NsrR, resulting in

222   inactivation of this repressor (15, 16). Many additional Fe-S cluster-containing proteins are

223   simultaneously damaged, so bacteria need to either repair damaged proteins or synthesize

224   replacement proteins, while simultaneously replenishing proteins that detoxify NO and prevent

225   further damage (17, 38). Although Fe-S cluster repair is likely required for bacterial survival, it

226   has been unclear whether or not this plays an important role within host tissues. We have chosen

227   to ask this question in a mouse model of *Y. pseudotuberculosis* infection, where it is known that

228   bacteria respond to RNS and that Fe concentrations are limiting (24, 25, 32).   *ytfE* expression

229   had been detected in *Yersinia* species replicating within host tissues, however it was unclear if

230   Fe-S cluster repair or assembly play a significant role during infection (36, 37). Here, we have

231   shown that Fe-S cluster repair contributes to successful *Y. pseudotuberculosis* replication within

232   the spleen.

233   We found that a place where Fe-S cluster repair in *Y. pseudotuberculosis* likely occurs is

234   in the peripheral subpopulation of bacteria that responds to NO assault within microcolonies.

235   This is consistent with a role for YftE in supporting survival of the peripheral subpopulation. In

236   the absence of *ytfE*, we would expect bacteria on the periphery to be exposed to stress associated

237   with NO exposure, leading to sequential loss of the peripheral population and progressively

238   smaller microcolonies. Consistent with this hypothesis, we observed Δ*ytfE* microcolonies were

239   smaller than those established by the WT strain. It is expected that the difference between WT

240   and Δ*ytfE* microcolony areas will become progressively more pronounced as the infection

12

241   proceeds, because Δ*ytfE* microcolonies should continuously lose their peripheral subpopulation.

242   This prediction is based on our previous observation that NO-sensitive microcolonies are

243   progressively reduced during the course of disease, with elimination of Δ*hmp* bacteria by NO

244   most pronounced at late timepoints post-inoculation, concurrent with a timepoint in which the

245   animals inoculated with the WT strain are moribund (32).

246   NO alone was not sufficient to limit the growth of Δ*ytfE* bacteria in bacteriological

247   media, consistent with previous studies that indicated the uropathogenic *E. coli* (UPEC) Δ*ytfE*

248   strain had reduced intracellular survival within host cells, but was not sensitive to exogenous NO

249   alone (39). Presumably, the Δ*ytfE* strain is sensitive to other antimicrobial compounds generated

250   within host tissues, possibly by the generation of a variety of reactive nitrogen species (RNS) as

251   a consequence of NO reaction with reactive oxygen species (ROS) or other compounds.

252   Upregulation of *ytfE* following hydrogen peroxide-mediated damage of *Staphylococcus aureus*

253   indicates that YtfE may play a broad role in repair, instead of just a response to nitrogen stress

254   (44, 45). Additional studies in *E. coli* also suggest that YtfE repairs Fe-S cluster proteins

255   damaged by hydrogen peroxide (13, 46-49).

256   An additional regulatory signal for the *yftE* gene is iron limitation, which depresses

257   synthesis of new Fe-S cluster proteins, thus requiring cellular YftE function (14, 21, 50). The

258   spleen is expected to be an iron-limiting environment requiring Fe-S cluster repair, but we found

259   no evidence for NO-independent induction of the *ytfE* gene within the center of microcolonies,

260   using our fluorescent promoter constructions. This contrasts with data arguing that *Y.*

261   *pseudotuberculosis* expresses many Fe acquisition genes during growth in host tissues, consistent

262   with Fe-limiting conditions within host tissues (25, 37). It is possible that the center of the

263   microcolony represents a protected environment with low exposure to stresses such as reactive

13

264   nitrogen and oxygen species as well as limited damage to Fe-S centers. Additionally, *ytfE*

265   expression may be induced at very low NO concentrations, as seen in *Salmonella enterica*

266   serovar Typhimurium (38), but may require severe iron limitation for expression in the absence

267   of NO.

268   The loss of YftE function also has the potential to alter metabolite levels due to

269   disruption of protein functions that are Fe-S center-related. In the presence of RNS, a Δ*ytfE*

270   strain may have reduced aconitase and fumarase activity due to the role of YtfE in Fe-S cluster

271   repair specifically for these proteins (47). The Fe-S cluster of the NsrR repressor is also repaired

272   by YtfE, which could lead to prolonged expression of the NsrR regulon in the presence of NO

273   (13). Our results indicate that expression of the NsrR regulon is similar in the presence or

274   absence of *ytfE*, although it remains possible that prolonged expression of the NsrR regulon

275   could be detected at later timepoints post-inoculation. Future work will investigate these issues,

276   and determine the interplay between iron regulation, NO-induced damage and repair of critical

277   Fe-S centers.

Materials and Methods

278

279   *Bacterial strains & growth conditions.* The WT *Y. pseudotuberculosis* strain, YPIII, was

280   used throughout. For all mouse infection experiments, bacteria were grown overnight to post-

281   exponential phase in 2xYT broth (LB, with 2x yeast extract and tryptone) at 26° C with rotation.

282   Exponential phase cultures were sub-cultured 1:100 from overnight cultures, and grown at 26° C

283   with rotation for an additional 2 hours. Sodium nitrite (2.5mM) was added to LB pH5.5 to

284   induce the nitrogen stress response. DETA-NONOate (2.5mM) NO donor compound (Cayman

285   Chemicals) was added to M9 minimal media to test NO sensitivity.

286   *Generation of ytfE mutant strains.* The *hmp* and *nsrR* deletion strains were previously

287   described (32). Deletion derivative strains were generated for *ytfE* by amplifying the start codon

288   + 3 downstream codons, the 3' terminal 3 codons + the stop codon and fusing these fragments to

289   generate a start + 6 aa + stop construct. Deletion constructions were amplified with 500 base

290   pairs flanking sequence on each side, cloned into the suicide vector, pSR47S, and transformed

291   into *Y. pseudotuberculosis*. Sucrose selection was used to select for bacteria that had

292   incorporated the desired mutation after a second cycle of recombination (31). PCR, sequencing,

293   and qRT-PCR were used to confirm deletion strains.

294   *Integrated ytfE reporter construction (ytfE*$^{+}$*rescue strain).* The *ytfE::gfp* reporter was

295   generated by cloning *gfp* immediately downstream of the *ytfE* gene (in between the *ytfE* stop

296   codon and terminator sequence) by overlap extension PCR. The *ytfE* start codon was amplified

297   with 500 base pairs upstream flanking sequence, while the stop codon of *gfp* was amplified with

298   500 base pairs downstream flanking sequence. This fragment was cloned into the suicide vector,

299   pSR47S, and transferred by conjugation into WT *Y. pseudotuberculosis hmp::mCherry*

300   (chromosomally integrated), selecting for kanamycin resistance. For the *ytfE*$^{+}$ rescue strain, a

15

301   WT *ytfE* gene product, including 500 base pairs upstream and downstream of *ytfE*, was amplified

302   from genomic DNA and cloned into pSR47S. This vector was transferred by conjugation into

303   Δ*ytfE Y. pseudotuberculosis*, selecting for kanamycin resistance. A second round of

304   recombination was selected on sucrose-containing media to isolate strains that had recombined

305   each *ytfE* construct. PCR and sequencing were used to confirm integration of *gfp* or rescue of

306   the *ytfE* deletion.

307   *Generation of plasmid-based reporter strains.* Several of the *Y. pseudotuberculosis*

308   reporter strains in this study have been previously described: WT GFP$^+$, WT mCherry$^+$

309   (*yopE::mCherry*), WT *hmp::mCherry*, WT GFP$^+$ *hmp::mCherry*, and Δ*hmp* GFP$^+$ (32). For this

310   study, GFP$^+$ strains were constructed by transforming deletion strains with the constitutive GFP

311   plasmid, which expresses GFP from an unrepressed P_{tet} of pACYC184. The P_{hmp}*::mCherry* was

312   also transformed into GFP$^+$ strains. The P_{hmp}*::mCherry* transcriptional fusion was previously

313   constructed by fusing the *hmp* promoter to *mCherry* using overlap extension PCR, and cloned

314   into the pMMB67EH plasmid (32).

315   *Murine model of systemic infection.* Six to 8-week old female C57BL/6 mice were

316   obtained from Jackson Laboratories (Bar Harbor, ME). All animal studies were approved by the

317   Institutional Animal Care and Use Committee of Tufts University. Mice were injected

318   intravenously with 10^3 bacteria for all experiments. For co-infection experiments, mice were

319   inoculated with 5×10^2 CFU of each strain, for a total of 10^3 CFUs. At the indicated timepoints

320   post-inoculation (PI) (3 days), spleens were removed and processed.

321   *qRT-PCR to detect bacterial transcripts in broth-grown cultures.* Bacterial cells were

322   grown in broth to $A_{600} = 0.3$ under appropriate stress conditions, pelleted, resuspended in Buffer

323   RLT (QIAGEN) + ß-mercaptoethanol, and RNA was isolated using the RNeasy kit (QIAGEN)

16

324   according to manufacturer's protocol. DNA contamination was eliminated using the DNA-free

325   kit (Ambion) according to manufacturer's protocol. RNA was reverse transcribed using M-MLV

326   reverse transcriptase (Invitrogen), in the presence of the RNase inhibitor, RnaseOUT

327   (Invitrogen), according to manufacturer's protocol. Approximately 30 ng cDNA was used as a

328   template in reactions with 0.5 µM of forward and reverse primers and SYBR Green (Applied

329   Biosystems) according to manufacturer's protocol. Control samples were prepared that lacked

330   M-MLV, to confirm DNA was eliminated from samples and was not amplified by qRT-PCR.

331   Reactions were carried out using the StepOnePlus Real-Time PCR system, and relative

332   comparisons were obtained using the $\Delta\Delta C_T$ or $2^{-\Delta Ct}$ method (Applied Biosystems).

333   *qRT-PCR to detect bacterial transcripts from mouse tissues.* Mice were inoculated

334   intravenously with the WT strain, and at day 3 PI spleens were harvested, and immediately

335   submerged in RNALater solution (QIAGEN). Tissue was homogenized in Buffer RLT + ß-

336   mercaptoethanol, and RNA was isolated using the RNeasy kit (QIAGEN) according to

337   manufacturer's protocol. Bacterial RNA was enriched following depletion of host mRNA and

338   rRNA from total RNA samples, using the MICROB*Enrich* kit (Ambion) according to

339   manufacturer's protocol. DNA digestion, reverse transcription, and qRT-PCR were performed

340   as described above.

341   *Fluorescence microscopy.* C57BL/6 mice were inoculated intravenously with the *Y.*

342   *pseudotuberculosis* WT strain, at day 3 PI spleens were harvested and immediately fixed in 4%

343   paraformaldehyde in PBS for 3 hours. Tissues were frozen-embedded in Sub Xero freezing

344   media (Mercedes Medical) and cut by cryostat microtome into 10µm sections. To visualize

345   reporters, sections were thawed in PBS, stained with Hoechst at a 1:10,000 dilution, washed in

346   PBS, and coverslips were mounted using ProLong Gold (Life Technologies). Tissue was imaged

347   with 20x or 63x objectives, using a Zeiss Axio Observer.Z1 (Zeiss) fluorescent microscope with

348   Colibri.2 LED light source, an Apotome.2 (Zeiss) for optical sectioning, and an ORCA-R^2 digital

349   CCD camera (Hamamatsu).

350   *Image analysis.* Volocity image analysis software was used to quantify microcolony

351   areas. Image J was used to quantify the signal intensity of each channel at the centroid and

352   periphery of each microcolony, to generate relative signal intensities of fluorescent reporters.

353   Thresholding was used to define the area of each microcolony, the centroid was calculated, and

354   0.01 pixel^2 squares were selected to calculate values at the centroid. Peripheral measurements

355   depict bacteria in contact with host cells.

356

357   **Author Contributions.** Designed and performed experiments: KMD, JK, SC.

358   Intellectual/conceptual contribution: KMD, RRI. Analyzed the data: KMD, JK, SC, RRI. Wrote

359   the paper: KMD, RRI.

360

368

18

369   **Figure Legends:**

370   **Figure 1**: *ytfE* **expression is regulated by NsrR and occurs within peripheral cells.** A)

371   C57BL/6 mice were inoculated intravenously (i.v.) with 10^3 WT *Y. pseudotuberculosis*, and

372   spleens were harvested at day 3 post-inoculation (PI). Bacterial transcripts were isolated from

373   splenic tissue, transcript levels were quantified by qRT-PCR relative to 16S, and the fold

374   increase in *ytfE* transcript levels is shown relative to the inoculum. Each dot represents an

375   individual mouse. B) Nitrogen stress was induced (NO_2, +) in cultures of WT and Δ*nsrR* strains,

376   and compared to untreated cultures (NO_2, -). The *ytfE* transcript levels are expressed relative to

377   16S, fold increase is relative to the average level in untreated WT cultures. Each column: 5

378   biological replicates, mean and SEM. C) C57BL/6 mice were inoculated i.v. with the WT

379   *hmp::mCherry ytfE::gfp* strain or the WT *yopE::mCherry ytfE;:gfp* strain, and spleens were

380   harvested at day 3 PI for fluorescence microscopy. Fluorescent signal intensity was determined

381   within the same peripheral and centroid cells for *hmp* and *ytfE* reporters or *yopE* and *ytfE*

382   reporters, and divided to generate the periphery/centroid ratio (4 mice/group). Dots: individual

383   microcolonies. D) Representative image of *hmp::mCherry* and *ytfE::gfp* reporters (top panels) or

384   *yopE::mCherry* and *ytfE::gfp* reporters (bottom panels); merge and single channel images are

385   shown. Scale bars: 20μm. Statistics: Wilcoxon matched pairs, **$p<0.01$, n.s.: not significant.

386

387   **Figure 2**: *ytfE* **contributes to growth in the spleen.** A) Co-infection with the WT and Δ*ytfE*

388   strains. C57BL/6 mice were inoculated i.v. with an equal mixture of mCherry$^+$ (*yopE::mCherry*)

389   WT and GFP$^+$ Δ*ytfE* strains, and spleens were harvested at day 3 PI. Competitive index: ratio of

390   Δ*ytfE*/WT CFUs in spleen at day 3, divided by ratio of Δ*ytfE*/WT CFUs in the inoculum. Dots:

391   individual mice. Dotted line: equal fitness, replicates completed on two separate days. B) WT

19

392 and $\Delta ytfE$ microcolony areas (μm^2) from the co-infection in panel 2A quantified (Experimental

393 Procedures) in 11 mice. C) C57BL/6 mice were inoculated i.v. with the WT GFP$^+$

394 *hmp::mCherry* or $\Delta ytfE$ GFP$^+$ *hmp::mCherry* strains, and spleens were harvested at day 3 PI for

395 fluorescence microscopy. Reporter signals were quantified within peripheral and centroid cells,

396 *hmp* reporter signal was divided by GFP. D) Representative image of a $\Delta ytfE$ GFP$^+$

397 *hmp::mCherry* microcolony, stained with Hoechst to detect host nuclei; merge and *hmp* single

398 channel images are shown Statistics: A): Wilcoxon Signed Rank Test, compared to a value of 1,

399 B): Mann-Whitney, C): Wilcoxon matched pairs, *$p<0.05$, ***$p<0.001$.

400

401 **Figure 3: $\Delta ytfE$ contributes to survival in the absence of *hmp*.** A) C57BL/6 mice were

402 inoculated i.v. with an equal mixture of *hmp* GFP$^+$ and Δhmp $\Delta ytfE$ GFP$^+$ P_{hmp}::*mCherry* strains,

403 and spleens were harvested at day 3 PI. Competitive index: ratio of Δhmp $\Delta ytfE$/Δhmp CFUs in

404 spleen at day 3, divided by ratio of Δhmp $\Delta ytfE$/Δhmp CFUs in the inoculum. Dots: individual

405 mice. Dotted line: represents equal fitness. Statistics: Wilcoxon Signed Rank Test, compared to

406 a value of 1, n.s.: not significant. B) Total CFUs in the spleen during co-infection, when CI was

407 less than 1 (Δhmp wins) or above or equal to 1 (Δhmp $\Delta ytfE$ wins). Dots: individual mice. C)

408 Δhmp and Δhmp $\Delta ytfE$ microcolony areas (μm^2) from the co-infection quantified (Experimental

409 Procedures) in 10 mice. Dots: individual microcolonies. D) Reporter signals were quantified

410 within peripheral and centroid cells in the Δhmp $\Delta ytfE$ strain during co-infection, *hmp* reporter

411 signal was divided by GFP. Dots: individual microcolonies. Statistics: B) and C): Mann-

412 Whitney, D): Wilcoxon matched pairs, *$p<0.05$, **$p<0.01$, n.s.: not significant.

413

20

414   **Figure 4: *ytfE* has limited effects on NO sensitivity in the absence of *hmp*.** A) Optical density

415   (A_{600nm}) was measured every 2 hours (time, hrs) within cultures of the indicated strains during

416   incubation in LB pH5.5 in the presence ($+NO_2$) and absence of $NaNO_2$. Data represents two

417   independent experiments. B) Optical density (A_{600nm}) was measured every 2 hours (time, hrs)

418   within cultures of the indicated strains during incubation in M9 minimal media in the presence

419   (+NO) and absence of the DETANONOate NO donor. Data represents three independent

420   experiments. C) C57BL/6 mice were inoculated i.v. with the Δ*ytfE* GFP$^+$ *P*$_{hmp}$*::mCherry* or

421   Δ*hmp* Δ*ytfE* GFP$^+$ *P*$_{hmp}$*::mCherry* strains, and spleens were harvested at day 3 PI for fluorescence

422   microscopy. Reporter signals were quantified within peripheral and centroid cells, *hmp* reporter

423   signal was divided by GFP. Dots: individual microcolonies. D) Representative images of Δ*ytfE*

424   and Δ*hmp* Δ*ytfE* microcolonies; merge and *hmp* single channel images are shown. Statistics:

425   Wilcoxon matched pairs, *p<0.05, n.s.: not significant.

426

427   **Figure 5: Rescue of *ytfE* restores fitness of the Δ*ytfE* strain.** A) C57BL/6 mice were

428   inoculated i.v. with an equal mixture of *ytfE* rescued GFP$^+$ and WT mCherry$^+$ strains, and spleens

429   were harvested at day 3 PI. Competitive index: ratio of *ytfE* rescue/WT CFUs in spleen at day 3,

430   divided by ratio of *ytfE* rescue/WT CFUs in the inoculum. Dots: individual mice. Dotted line:

431   equal fitness, replicates completed on two separate days. Statistics: Wilcoxon Signed Rank Test,

432   compared to a value of 1, n.s.: not significant. B) WT and *ytfE* rescue microcolony areas (μm^2)

433   from the co-infection quantified (Experimental Procedures) in 10 mice. Dots: individual

434   microcolonies. C) Representative images of WT mCherry$^+$ and *ytfE* rescued GFP$^+$ microcolonies.

435   Scale bar: 20μm. Statistics: Mann-Whitney, n.s.: not significant.

References

1.   Bogdan C. Nitric oxide and the immune response. Nat Immunol. 2001;2(10):907-16.

2.   Nathan C. Nitric oxide as a secretory product of mammalian cells. FASEB J. 1992;6(12):3051-64.

3.   Pervin S, Singh R, Hernandez E, Wu G, Chaudhuri G. Nitric oxide in physiologic concentrations targets the translational machinery to increase the proliferation of human breast cancer cells: involvement of mammalian target of rapamycin/eIF4E pathway. Cancer Res. 2007;67(1):289-99.

4.   Pervin S, Singh R, Chaudhuri G. Nitric oxide-induced cytostasis and cell cycle arrest of a human breast cancer cell line (MDA-MB-231): potential role of cyclin D1. Proc Natl Acad Sci. 2001;98(6):3583-8.

5.   Dubey M, Nagarkoti S, Awasthi D, Singh A, Chandra T, Kumaravelu J, et al. Nitric oxide-mediated apoptosis of neutrophils through caspase-8 and caspase-3-dependent mechanism. Cell Death Dis. 2016;7(9):e2348.

6.   Kumar S, Barthwal M, Dikshit M. Cdk2 nitrosylation and loss of mitochondrial potential mediate NO-dependent biphasic effect on HL-60 cell cycle. Free Radic Biol Med. 2010;48(6):851-61.

7.   Kobayashi Y. The regulatory role of nitric oxide in proinflammatory cytokine expression during the induction and resolution of inflammation. J Leukoc Biol. 2010;88(6):1157-62.

8.   Zeigler M, Doseff A, Galloway M, Opalek J, Nowicki P, Zweier J, et al. Presentation of nitric oxide regulates monocyte survival through effects on caspase-9 and caspase-3 activation. J Biol Chem. 2003;278(15):12894-902.

9.   Pautz A, Art J, Hahn S, Nowag S, Voss C, Kleinert H. Regulation of the expression of inducible nitric oxide synthase. Nitric Oxide. 2010;23(2):75-93.

10.   Fang F. Perspective series: host/pathogen interactions. Mechanisms of nitric oxide-related antimicrobial activity. J Clin Invest. 1997;99(12):2818-25.

462   11.   Pullan S, Gidley M, Jones R, Barrett J, Stevanin T, Read R, et al. Nitric oxide in
463   chemostat-cultured *Escherichia coli* is sensed by Fnr and other global regulators: unaltered
464   methionine biosynthesis indicates lack of S nitrosation. J Bacteriol. 2007;189(5):1845-55.

465   12.   Gilberthorpe N, Lee M, Stevanin T, Read R, Poole R. NsrR: a key regulator
466   circumventing *Salmonella enterica* serovar Typhimurium oxidative and nitrosative stress *in vitro*
467   and in IFN-gamma-stimulated J774.2 macrophages. Microbiology. 2007;153(6):1756-71.

468   13.   Overton T, Justino M, Li Y, Baptista J, Melo A, Cole J, et al. Widespread distribution in
469   pathogenic bacteria of di-iron proteins that repair oxidative and nitrosative damage to iron-sulfur
470   clusters. J Bacteriol. 2008;190(6):2004-13.

471   14.   Bodenmiller D, Spiro S. The yjeB (nsrR) gene of *Escherichia coli* encodes a nitric oxide-
472   sensitive transcriptional regulator. J Bacteriol. 2006;188(3):874-81.

473   15.   Tucker N, Hicks M, Clarke T, Crack J, Chandra G, Le Brun N, et al. The transcriptional
474   repressor protein NsrR senses nitric oxide directly via a [2Fe-2S] cluster. PLoS ONE.
475   2008;3(11):e3623.

476   16.   Volbeda A, Dodd E, Darnault C, Crack J, Renoux O, Hutchings M, et al. Crystal
477   structures of the NO sensor NsrR reveal how its iron-sulfur cluster modulates DNA binding. Nat
478   Commun. 2017;8:15052.

479   17.   Filenko N, Spiro S, Browning D, Squire D, Overton T, Cole J, et al. The NsrR regulon of
480   *Escherichia coli* K-12 includes genes encoding the hybrid cluster protein and the periplasmic,
481   respiratory nitrite reductase. J Bacteriol. 2007;189(12):4410-7.

482   18.   Partridge J, Bodenmiller D, Humphrys M, Spiro S. NsrR targets in the *Escherichia coli*
483   genome: new insights into DNA sequence requirements for binding and a role for NsrR in the
484   regulation of motility. Mol Microbiol. 2009;73(4):680-94.

485   19.   Robinson J, Brynildsen M. A kinetic platform to determine the fate of nitric oxide in
486   *Escherichia coli*. PLoS Comput Biol. 2013;9(5):e103049.

487   20.   Poole R, Anjum M, Membrillo-Hernández J, Kim S, Hughes M, Stewart V. Nitric oxide,
488   nitrite, and Fnr regulation of *hmp* (flavohemoglobin) gene expression in *Escherichia coli* K-12. J
489   Bacteriol. 1996;178(18):5487-92.

490   21.   Justino M, Almeida C, Gonçalves V, Teixeira M, Saraiva L. *Escherichia coli* YtfE is a
491   di-iron protein with an important function in assembly of iron-sulphur clusters. FEMS Microbiol
492   Lett. 2006;257(2):278-84.

493   22.   Todorovic S, Justino M, Wellenreuther G, Hildebrandt P, Murgida D, Meyer-Klaucke W,
494   et al. Iron-sulfur repair YtfE protein from *Escherichia coli*: structural characterization of the di-
495   iron center. J Biol Inorg Chem. 2008;13(5):765-70.

496   23.   Miller H, Kwuan L, Schwiesow L, Bernick D, Mettert E, Ramirez H, et al. IscR is
497   essential for *Yersinia pseudotuberculosis* type III secretion and virulence. PLoS Pathog.
498   2014;10(6):e1004194.

499   24.   Miller H, Schwiesow L, Au-Yeung W, Auerbuch V. Hereditary hemochromatosis
500   predisposes mice to *Yersinia pseudotuberculosis* infection even in the absence of the type III
501   secretion system. Front Cell Infect Microbiol. 2016;6:69.

502   25.   Schwiesow L, Mettert E, Wei Y, Miller H, Herrera N, Balderas D, et al. Control of *hmu*
503   heme uptake genes in *Yersinia pseudotuberculosis* in response to iron sources. Front Cell Infect
504   Microbiol. 2018;8:47.

505   26.   Hubbert W, Petenyi C, Glasgow L, Uyeda C, Creighton S. *Yersinia pseudotuberculosis*
506   infection in the United States. Septicemia, appendicitis, and mesenteric lymphadenitis. Am J
507   Trop Med Hyg. 1971;20(5):679-84.

508   27.   Gurry J. Acute terminal ileitis and yersinia infection. Br Med J. 1974;2(5913):264-6.

509   28.   Capron J, Delamarre J, Delcenserie R, Gineston J, Dupas J, Lorriaux A. Liver absess
510   complicating *Yersinia pseudotuberculosis* ileitis. Gastroenterology. 1981;81(1):150-2.

511   29.   Paff J, Triplett D, Saari T. Clinical and laboratory aspects of *Yersinia pseudotuberculosis*
512   infections, with a report of two cases. Am J Clin Pathol. 1976;66(1):101-10.

513   30.   Barnes P, Bergman M, Mecsas J, Isberg R. *Yersinia pseudotuberculosis* disseminates
514   directly from a replicating bacterial pool in the intestine. J Exp Med. 2006;203(6):1591-601.

515   31.   Crimmins G, Mohammadi S, Green E, Bergman M, Isberg R, Mecsas J. Identification of
516   MrtAB, an ABC transporter specifically required for *Yersinia pseudotuberculosis* to colonize the
517   mesenteric lymph nodes. PLoS Pathog. 2012;8(8):e1002828.

518   32.   Davis K, Mohammadi S, Isberg R. Community behavior and spatial regulation within a
519   bacterial microcolony in deep tissue sites serves to protect against host attack. Cell Host
520   Microbe. 2015;17(1):21-31.

521   33.   Zhang Y, Khairallah C, Sheridan B, van der Velden A, Bliska J. CCR2+ inflammatory
522   monocytes are recruited to *Yersinia pseudotuberculosis* pyogranulomas and dictate adaptive
523   responses at the expense of innate immunity during oral infection. Infect Immun.
524   2018;86(3):e00782-17.

525   34.   Peterson L, Philip N, DeLaney A, Wynosky-Dolfi M, Asklof K, Gray F, et al. RIPK1-
526   dependent apoptosis bypasses pathogen blockage of innate signaling to promote immune
527   defense. J Exp Med. 2017;214(11):3171-82.

528   35.   Durand E, Maldonado-Arocho F, Castillo C, Walsh R, Mecsas J. The presence of
529   professional phagocytes dictates the number of host cells targeted for Yop translocation during
530   infection. Cell Microbiol. 2010;12(8):1064-82.

531   36.   Sebbane F, Lemaître N, Sturdevant D, Rebeil R, Virtaneva K, Porcella S, et al. Adaptive
532   response of *Yersinia pestis* to extracellular effectors of innate immunity during bubonic plague.
533   Proc Natl Acad Sci. 2006;103(31):11766-71.

534   37.   Nuss A, Beckstette M, Pimenova M, Schmühl C, Opitz W, Pisano F, et al. Tissue dual
535   RNA-seq allows fast discovery of infection-specific functions and riboregulators shaping host-
536   pathogen transcriptomes. Proc Natl Acad Sci. 2017;114(5):E791-E800.

537   38.   Karlinsey J, Bang I, Becker L, Frawley E, Porwollik S, Robbins H, et al. The NsrR
538   regulon in nitrosative stress resistance of *Salmonella enterica* serovar Typhimurium. Mol
539   Microbiol. 2012;85(6):1179-93.

540   39.   Shepherd M, Achard M, Idris A, Totsika M, Phan M, Peters K, et al. The cytochrome bd-
541   I respiratory oxidase augments survival of multidrug-resistant *Escherichia coli* during infection.
542   Sci Rep. 2016;6:35285.

543   40.   Shiloh M, MacMicking J, Nicholson S, Brause J, Potter S, Marino M, et al. Phenotype of
544   mice and macrophages deficient in both phagocyte oxidase and inducible nitric oxide synthase.
545   Immunity. 1999;10(1):29-38.

546   41.   Vasquez-Torres A, Jones-Carson J, Mastroeni P, Ischiropoulos H, Fang F. Antimicrobial
547   actions of the NADPH phagocyte oxidase and inducible nitric oxide synthase in experimental

25

548   salmonellosis. I. Effects on microbial killing by activated peritoneal macrophages in vitro. J Exp
549   Med. 2000;192(2):227-36.

550   42.   Shiloh M, Nathan C. Reactive nitrogen intermediates and the pathogenesis of *Salmonella*
551   and *Mycobacteria*. Curr Opin Microbiol. 2000;3(1):35-42.

552   43.   Bang I, Liu L, Vasquez-Torres A, Crouch M, Stamler J, Fang F. Maintenance of nitric
553   oxide and redox homeostasis by the *Salmonella* flavohemoglobin *hmp*. J Biol Chem.
554   2006;281(38):28039-47.

555   44.   Mashruwala A, Boyd J. The *Staphylococcus aureus* SrrAB regulatory system modulates
556   hydrogen peroxide resistance factors, which imparts protection to aconitase during aerobic
557   growth. PLoS ONE. 2017;12(1):e0170283.

558   45.   Kinkel T, Roux C, Dunman P, Fang F. The *Staphylococcus aureus* SrrAB two-
559   component system promotes resistance to nitrosative stress and hypoxia. MBio.
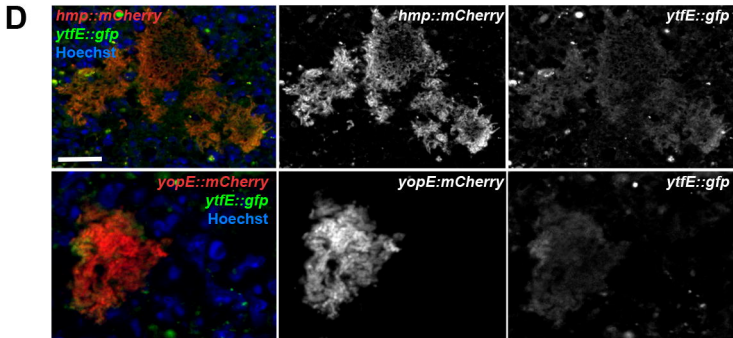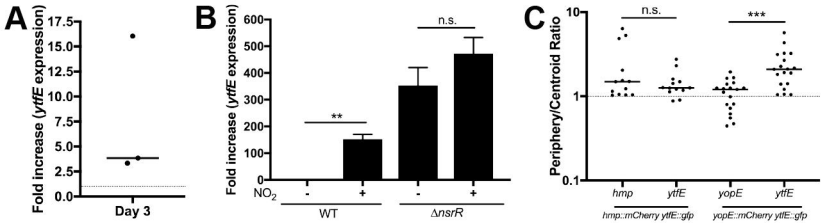560   2013;4(6):e00696-13.

561   46.   Jang S, Imlay J. Micromolar intracellular hydrogen peroxide disrupts metabolism by
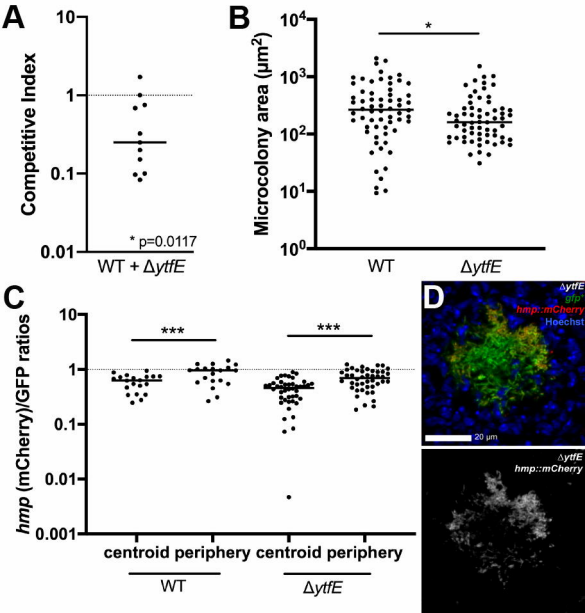562   damaging iron-sulfur enzymes. J Biol Chem. 2007;282(2):929-37.

563   47.   Justino M, Almeida C, Teixeira M, Saraiva L. *Escherichia coli* di-iron YtfE protein is
564   necessary for the repair of stress-damaged iron-sulfur clusters. J Biol Chem.
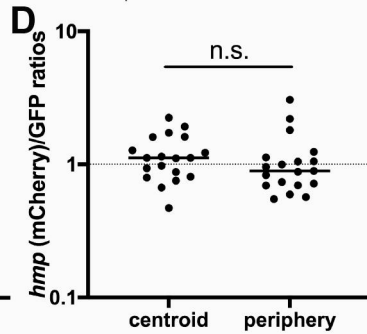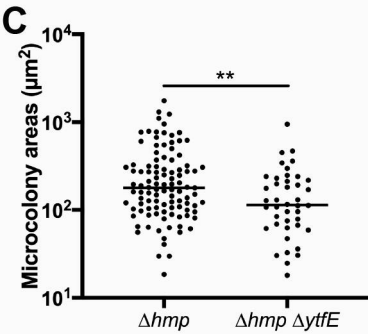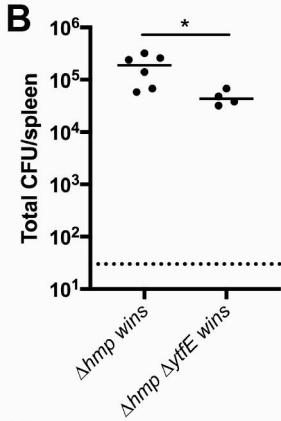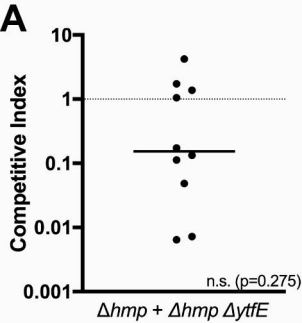565   2007;282(14):10352-9.

566   48.   Velayudhan J, Karlinsey J, Frawley E, Becker L, Nartea M, Fang F. Distinct roles of the
567   *Salmonella enterica* serovar Typhimurium CyaY and YggX proteins in the biosynthesis and
568   repair of iron-sulfur clusters. Infect Immun. 2014;82(4):1390-401.

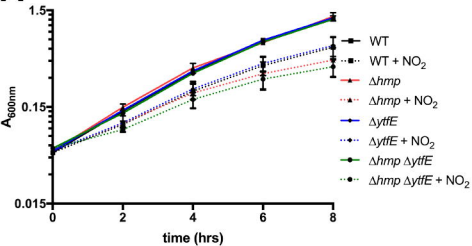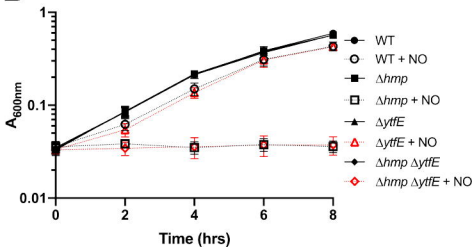569   49.   Silva L, Baptista J, Batley C, Andrews S, Saraiva L. The di-iron RIC protein (YtfE) of
570   *Escherichia coli* interacts with the DNA-binding protein from starved cells (Dps) to diminish
571   RIC protein-mediated redox stress. J Bacteriol. 2018;200(24):e00527-18.

572   50.   Djaman O, Outten F, Imlay J. Repair of oxidized iron-sulfur clusters in *Escherchia coli*. J
573   Biol Chem. 2004;279(43):44590-99.
574

26

A Fold increase (*ytfE* expression) — Day 3

B Fold increase (*ytfE* expression) — NO$_2$ − + − +, WT, Δ*nsrR*; ** n.s.

C Periphery/Centroid Ratio — *hmp*, *ytfE*, *yopE*, *ytfE*; *hmp::mCherry ytfE::gfp*, *yopE::mCherry ytfE::gfp*; n.s. ***

D *hmp::mCherry* *ytfE::gfp* Hoechst | *hmp::mCherry* | *ytfE::gfp*
yopE::mCherry *ytfE::gfp* Hoechst | *yopE:mCherry* | *ytfE::gfp*

A Competitive Index

* p=0.0117

WT + Δ*ytfE*

B Microcolony area (μm²)

*

WT   Δ*ytfE*

C *hmp* (mCherry)/GFP ratios

***   ***

centroid periphery   centroid periphery

WT   Δ*ytfE*

D
Δ*ytfE*
gfp
hmp::mCherry
Hoechst

20 μm

Δ*ytfE*
hmp::mCherry

A Competitive Index

Δhmp + Δhmp ΔytfE

n.s. (p=0.275)

B Total CFU/spleen

Δhmp wins   Δhmp ΔytfE wins

*

C Microcolony areas (µm²)

Δhmp   Δhmp ΔytfE

**

D hmp (mCherry)/GFP ratios

centroid   periphery

n.s.

A

B

C

D

A — Competitive Index (WT + *ytfE* rescue); n.s. (p=0.922)

B — Microcolony areas (μm^2) for WT vs *ytfE* rescue; n.s.

C — WT; *ytfE* rescue